



## Original Full Length Article

## The role of bone intrinsic properties measured by infrared spectroscopy in whole lumbar vertebra mechanics: Organic rather than inorganic bone matrix?

Julien Wegrzyn<sup>a,b,\*</sup>, Jean-Paul Roux<sup>a,1</sup>, Delphine Farlay<sup>a,1</sup>, H el ene Follet<sup>a</sup>, Roland Chapurlat<sup>a</sup>

<sup>a</sup> INSERM, UMR 1033, Universit e de Lyon, Lyon, France

<sup>b</sup> Department of Orthopedic Surgery – Pavillon T, H opital Edouard Herriot, Lyon, France

## ARTICLE INFO

## Article history:

Received 4 February 2013

Revised 24 May 2013

Accepted 10 June 2013

Available online xxxx

Edited by: David Burr

## Keywords:

Bone mechanics

Vertebra

Bone matrix

Collagen maturity

Bone microarchitecture

## ABSTRACT

Whole bone strength is determined by bone mass, microarchitecture and intrinsic properties of the bone matrix. However, few studies have directly investigated the contribution of bone tissue material properties to whole bone strength in humans. This study assessed the role of bone matrix composition on whole lumbar vertebra mechanics. We obtained 17 fresh frozen human lumbar spines (8 W, 9 M, aged  $76 \pm 11$  years). L3 bone mass was measured by DXA and microarchitecture by  $\mu$ -CT with a  $35 \mu\text{m}$ -isotropic resolution. Microarchitectural parameters were directly measured: Tb.BV/TV, SMI, Tb.Th, DA, Ct.Th, Ct.Po and radius of anterior cortical curvature. Failure load (N), stiffness (N/mm) and work to failure (N.mm) were extracted from quasi-static uniaxial compressive testing performed on L3 vertebral bodies. FTIRM analysis was performed on  $2 \mu\text{m}$ -thick sections from L2 trabecular cores, with a Perkin-Elmer GXII Auto-image Microscope equipped with a wide band detector. Twenty measurements per sample were performed at  $30 \times 100 \mu\text{m}$  of spatial resolution. Each spectrum was collected at  $4 \text{ cm}^{-1}$  resolution and 50 scans in transmission mode. Mineral and collagen maturity, and mineralization and crystallinity index were measured. There was no association between the bone matrix characteristics and bone mass or microarchitecture. Mineral maturity, mineralization and crystallinity index were not related to whole vertebra mechanics. However, collagen maturity was positively correlated with whole vertebra failure load and stiffness ( $r = 0.64$ ,  $p = 0.005$  and  $r = 0.54$ ,  $p = 0.025$ , respectively). The collagen maturity (3rd step) in combination with bone mass (i.e. BMC, 1st step) and microarchitecture (i.e. Tb.Th, 2nd step) improved the prediction of whole vertebra mechanical properties in forward stepwise multiple regression models, together explaining 71% of the variability in whole vertebra stiffness ( $p = 0.001$ ). In conclusion, we demonstrated a substantial contribution of collagen maturity, but not mineralization parameters, to whole bone strength of human lumbar vertebrae that was independent of bone mass and microarchitecture.

  2013 Published by Elsevier Inc.

## Introduction

Mechanical principles dictate that whole bone strength is determined by bone mass, bone microarchitecture and intrinsic properties of the bone matrix [1,2]. Beside bone mass, the contribution of microarchitecture and its spatial distribution (i.e.; microarchitecture heterogeneity) has been extensively explored biomechanically and clinically. It is probably the best understood among the different levels of analysis [3–7]. Specifically, impairment in trabecular and cortical microarchitecture impacts dramatically on whole bone strength and the risk of fragility fracture, independently of areal bone mineral density (aBMD) [3,4]. In addition, the post-fracture mechanical behavior of vertebrae after initial mild fracture was demonstrated ex-vivo to be related to bone microarchitecture but

not bone mass [5]. Abnormalities in age-related enzymatic and non-enzymatic collagen cross-links affect the mineralization process, and can lead to microdamage accumulation and impaired bone mechanical behavior therefore contributing to fracture risk prediction. However, the direct contribution of bone matrix properties to bone strength is more difficult to assess and therefore, remains poorly understood at the whole bone level in humans [2,8–11]. Micro- or nano-indentation techniques in human iliac bone samples demonstrated a strong relationship between the bone matrix and local tissue mechanical behavior [12,13]. Along with mineralized matrix, the organic matrix accounts for one third of the variance in bone microhardness at the bone structural unit level [12]. Particularly, collagen maturity explained plastic mechanical properties whereas elastic mechanical properties were explained by mineralization [13]. In addition, at the whole-bone level in rat humerus, bone tissue material composition was a strong predictor of mechanical behavior, accounting for up to 83% of the variability in bone mechanics [14]. Therefore, the mechanical properties of the bone matrix are important parameters to explore to enhance the understanding of

\* Corresponding author at: Department of Orthopedic Surgery – Pavillon T, H opital Edouard Herriot, 5, Place d'Arsonval, 69437 Lyon, France. Fax: +33 4 72 11 76 37.

E-mail address: [julien.wegrzyn@chu-lyon.fr](mailto:julien.wegrzyn@chu-lyon.fr) (J. Wegrzyn).

<sup>1</sup> These authors contributed equally to this work.

mechanisms involved in bone fragility. For example, in cohort studies, bisphosphonates impacted on bone matrix formation, in addition to their well-established antiresorptive effect. They contribute, therefore, to fragility fracture prevention and highlight the necessity for assessment of the bone matrix contribution to whole bone strength [15,16].

This study aimed to investigate the direct contribution of the organic and inorganic bone matrix properties to the mechanical behavior of whole human lumbar vertebrae. We hypothesized that bone matrix directly impacts mechanical behavior at the whole bone level, independently of bone mass and microarchitecture.

## Material and methods

### Bone specimens

Lumbar spines (L1–L5) were harvested fresh from 17 Caucasian elderly human donors (8 women and 9 men) aged  $76 \pm 11$  years-old. Source of the donors was anatomical donation and their available medical history was limited to the cause of the death. The absence of prevalent fractures or significant bone diseases involving the lumbar spine (i.e., bone metastasis, Paget's disease, or Kellgren–Lawrence grades 3 and 4 lumbar spine osteoarthritis) was assessed using high-resolution lateral radiographs of the whole lumbar spine (Faxitron X-ray Corp., Lincolnshire, IL, USA). Then, the L2 and L3 vertebrae were separated from the lumbar spines and frozen at  $-20^\circ\text{C}$  wrapped in saline-soaked gauze. Bone mass, trabecular and cortical microarchitecture and bone mechanics were measured on the L3 vertebrae [3–5]. The organic and inorganic trabecular bone matrix properties were assessed on the L2 vertebrae using Fourier transform infrared microspectroscopy (FTIRM) [17].

### Bone mass and microarchitecture assessment

After thawing at room temperature, bone mineral content (BMC, g) and areal lateral bone mineral density (aBMD,  $\text{g}/\text{cm}^2$ ) of the L3 vertebrae was measured using dual-energy X-ray absorptiometry (DXA; Delphi W, Hologic, Waltham, MA, USA). Then, the posterior arches and surrounding soft tissues including the intervertebral disks were carefully removed. Microarchitecture was measured using a  $\mu$ -CT device (Skyscan 1076, Aartselaar, Belgium) on L3 vertebral bodies immersed in Ashman's solution. A nominal isotropic voxel size of  $35\ \mu\text{m}$  was used (field of view  $70\ \text{mm}$ ,  $2000 \times 2000$  pixels, X-ray source:  $100\ \text{kV}$ – $100\ \mu\text{A}$ ). Two- to three-dimension processing, analysis and visualization were performed using Skyscan Ant@ software. The following microarchitectural parameters were directly measured: trabecular bone volume per tissue volume (Tb.BV/TV, %), trabecular thickness (Tb.Th, mm), structure model index (SMI, #), degree of anisotropy (DA, #), anterior cortical thickness (Ct.Th, mm) and porosity (Ct.Po, %), and anterior cortical radius of curvature (Ct.Curv, mm).

### Mechanical testing

After  $\mu$ -CT acquisition, L3 vertebral bodies were kept moist at  $+4^\circ\text{C}$  with Ashman's solution until mechanical testing. A polyester resin interface (Soloplast V11, Vosschemie, Saint-Egrève, France) with a quick-setting polymerization at low temperature (maximum exothermic peak  $< +40^\circ\text{C}$ ) was applied to each endplate of the L3 vertebral body to achieve parallel surfaces for load application. Then, quasi-static uniaxial compressive testing was performed on the whole vertebral body submerged in  $+37^\circ\text{C}$ -controlled Ashman's solution using a screw-driven testing machine (Schenck RSA-250, Darmstadt, Germany) under displacement control at  $0.5\ \text{mm}/\text{mm}$  until failure. The compressive load and displacement were measured, respectively, using a  $5000\ \text{N}$  load cell (F 501 TC, TME, Signes, France) and a displacement transducer mounted directly on the vertebral resin endplates (Mecanium mechanical engineering, Lyon, France). Preconditioning was performed prior to testing (10 cycles with

loading at  $100\ \text{N}$  and unloading at  $50\ \text{N}$ ). The following parameters were determined from the load-displacement data: failure load (N), defined by the force at the maximum on the load-displacement curve, stiffness (N/mm), defined by the linear part of load-displacement curve slope between 25% and 75% of the failure load and, work to failure (N.mm), defined by the area under the load-displacement curve to the failure load.

### FTIRM (Fourier Transform InfraRed Microspectroscopy) analysis of bone matrix

L2 vertebrae were sectioned in half using an Isomet Buehler 4000 micro-saw (Buehler GmbH, Düsseldorf, Germany). A cylindrical core sample of trabecular bone was removed in the cranio-caudal direction from the anterior quadrant of the right half of vertebrae using an  $8.25\ \text{mm}$ -diameter diamond tipped coring tool. The end plate of each core was removed with the micro-saw. Trabecular cores were fixed in 70% ethanol for 2 weeks, dehydrated for 48 h in absolute alcohol, substituted in methylcyclohexane for 48 h and then embedded in polymethylmethacrylate (PMMA). FTIRM was performed in transmission mode on  $2\ \mu\text{m}$ -thick sections with a Perkin-Elmer GXII Auto-image Microscope (Norwalk, CT, USA) equipped with a wideband detector (mercury-cadmium-telluride) ( $7800$ – $400\ \text{cm}^{-1}$ ). A Cassegrain objective with numerical aperture of 0.6 was used with a spatial resolution of  $10\ \mu\text{m}$  at typical mid-infrared wavelengths. Twenty measurements per sample were done at  $30 \times 100\ \mu\text{m}$  of spatial resolution to cover the whole surface of the vertebral trabecular core. Each spectrum was collected at  $4\ \text{cm}^{-1}$  resolution and 50 scans by spectrum in the transmission mode. Contribution of air and PMMA were subtracted from the original spectrum. After automatic baseline correction (Spectrum Software) and curve fitting of every individual spectrum, GRAMS/AI software (Thermo Galactic, Salem, NH, USA) was used to quantify the characteristics of the spectra (Fig. 1). The following parameters were determined: the mineral crystallinity index which is inversely proportional to the full width at half-maximum of the  $604\ \text{cm}^{-1}$  peak (apatitic phosphate environment) and corresponds to both crystal size and perfection [18], the mineralization index which is the area ratio of the bands of mineral matrix over organic matrix ( $1184$ – $910\ \text{cm}^{-1}$ / $1712$ – $1592\ \text{cm}^{-1}$ ) [17], the mineral maturity which is calculated as the area ratio of the apatitic phosphate over nonapatitic phosphate ( $1030/1110\ \text{cm}^{-1}$  area ratio) and reflects the age of mineral [18], and the collagen maturity which is calculated as the ratio of organic matrix bands ( $1660/1690\ \text{cm}^{-1}$  area ratio) [18] and reflects the change in secondary structure of collagen in relation to the mineralization process [19] (Fig. 1).

### Statistical analyses

Shapiro–Wilk tests were used to assess the normality of the distributions. For Ct.Th, Ct.Po, Ct.Curv and work to failure, distributions

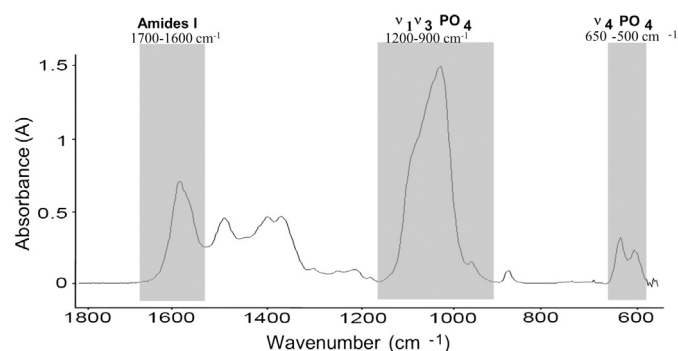


Fig. 1. Typical FTIRM spectra characteristics of a L2 core biopsy showing the peaks of amides ( $1600$ – $1700\ \text{cm}^{-1}$ ) of the  $\nu_4\text{PO}_4$  domain ( $500$ – $650\ \text{cm}^{-1}$ ) and of the  $\nu_1\nu_3\text{PO}_4$  domain ( $900$ – $1200\ \text{cm}^{-1}$ ).

Download English Version:

<https://daneshyari.com/en/article/5890939>

Download Persian Version:

<https://daneshyari.com/article/5890939>

[Daneshyari.com](https://daneshyari.com)